Electronic Supplementary Material (ESI) for Journal of Materials Chemistry C.

Quantitative model of multi-scale single quantum dot blinking

Supplementary Information

Eduard A. Podshivaylov,[†] Maria A. Kniazeva,[‡,¶] Alexander O. Tarasevich,[¶] Ivan Yu. Eremchev,[§] Andrei V. Naumov,[§,¶,‖] and Pavel A. Frantsuzov[*,†]

†*Voevodsky Institute of Chemical Kinetics and Combustion SB RAS, Novosibirsk, 630090 Russia*

‡*HSE University, Moscow, 101000 Russia*

¶*Lebedev Physical Institute of the Russian Academy of Sciences, Troitsk Branch, Moscow, 108840 Russia*

§*Institute of Spectroscopy of the Russian Academy of Sciences, Moscow, 108840 Russia*

‖*Moscow Pedagogical State University (MPGU), Moscow, 119435 Russia*

E-mail: frantsuzov@kinetics.nsc.ru

Contents

Supplementary note 1: Fluorescence lifetime intensity distribution

In the experiment a single quantum dot is excited by laser pulses with the repetition period of $T_r = 10^{-6}s$. The power of the each pulse is $P[Jcm^{-2}]$. The mean number of the photons absorbed by the QD after one pulse is:

$$N_a = \frac{P\sigma_a}{\hbar\omega} \tag{1}$$

where σ_a is the QD absorption cross-section and $\hbar\omega$ is the excitation photon energy. The measuring system detects single photons emitted by the QD. In the experiment $N_a \ll 1$ so the probability of a double excitation of the QD is very low. In this case the emission properties of the single quantum dot over time can be characterized by the instantaneous photoluminescence quantum yield (PLQY) $Y(t)$. It is defined as the probability that a quantum dot will emit a photon when excited at time t. Thus, the mean number of photons detected after the excitation pulse at time t is:

$$N_p(t) = \alpha Y(t) N_a + N_b \tag{2}$$

where α is the efficiency of the optical system and N_b is the mean number of background photons.

The instantaneous quantum yield can not be measured directly. Instead we can find the total number of photons detected within one bin which starts at time t and has the duration of $\Delta t \gg T_r$:

$$N = \int_t^{t+\Delta t} n_d(t')\, dt' \tag{3}$$

where the density of the detected photons n_d is defined as:

$$n_d(t) = \sum_{i=1}^{N} \delta(t - t_i) \tag{4}$$

and t_i is the i-th photon detection time. From Eq. (2) the mean number of the detected photons per bin can be expressed in terms of the instantaneous photoluminescence quantum yield:

$$\overline{N} = A\overline{Y} + b \tag{5}$$

where $\overline{Y}$ is average PLQY value over the duration of the bin:

$$\overline{Y} = \int_{t}^{t+\Delta t} Y_t(t')\, dt' \tag{6}$$

Coefficient A is:

$$A = \alpha N_a \frac{\Delta t}{T_r} \tag{7}$$

and b is mean number of the background photons per bin:

$$b = \frac{\Delta t}{T_r} N_b \tag{8}$$

The local fluorescence lifetime can be estimated within the same experiment by collecting the set of the delay times of the photon detections Δt_i defined as the difference of t_i and the time of the latest pulse before it. That allows us to calculate the fluorescence lifetime - intensity distribution (FLID) for each single QD.

The following procedure was used. We collected delay times within several bins having the same N value so that the number of times collected was at least 250. The measured delay times in the experiment were discretized with a step of δ. In our experiments the discretization time was 164.6 ps. Thus the collection of the delay times has the form of a histogram $n_1, n_2, \ldots$ where n_i is the number of delay times within an interval from $(i-1)\delta$

to $i\delta$. Each set of delay times was fitted with the double exponential probability distribution with a background:

$$P_i = \frac{A_1}{\tau_1} \exp\left(-\frac{i\delta}{\tau_1}\right) + \frac{A_2}{\tau_2} \exp\left(-\frac{i\delta}{\tau_2}\right) + c \tag{9}$$

which has five parameters A_1, A_2, τ_1, τ_2, and c. Only four of them are independent. The fifth parameter (we chose A_2) can be found from the normalization condition:

$$\sum_i P_i = 1 \tag{10}$$

We used the maximum likelihood method for fitting. The logarithm of the likelihood function (multinomial probability function) is given by the following expression:

$$\ln L(\tau_1, \tau_2, A_1, c) = \sum_i n_i \ln P_i(\tau_1, \tau_2, A_1, c) + \ln L_0 \tag{11}$$

where L_0 does not depend on the fitting parameters. Maximizing the likelihood function, we obtain τ_1 and τ_2 and set the minimum of them as the fluorescence lifetime estimator $\hat{\tau}$. The distribution of the pairs $(\hat{\tau}, N)$ generates a FLID plot. The FLID plots for all studied QDs are shown in Fig. (S1). We can see that all of the FLID plots show a nearly linear dependence.

This is evidence that the blinking is proceeding according to the trapping mechanism,[1,2] which predicts:

$$Y(t) = \frac{k_r}{k_r + k_t(t)} \equiv k_r \tau(t) \tag{12}$$

where k_r is the radiative recombination rate, and k_t is the trapping rate. Averaging this equation over the duration of the bin we get:

$$\overline{Y} = k_r \overline{\tau} \tag{13}$$

Substituting to Eq. (5)

$$\overline{N} = Ak_r\overline{\tau} + b \tag{14}$$

The mean number of detected photons linearly depends on the average fluorescence lifetime within the trapping mechanism.

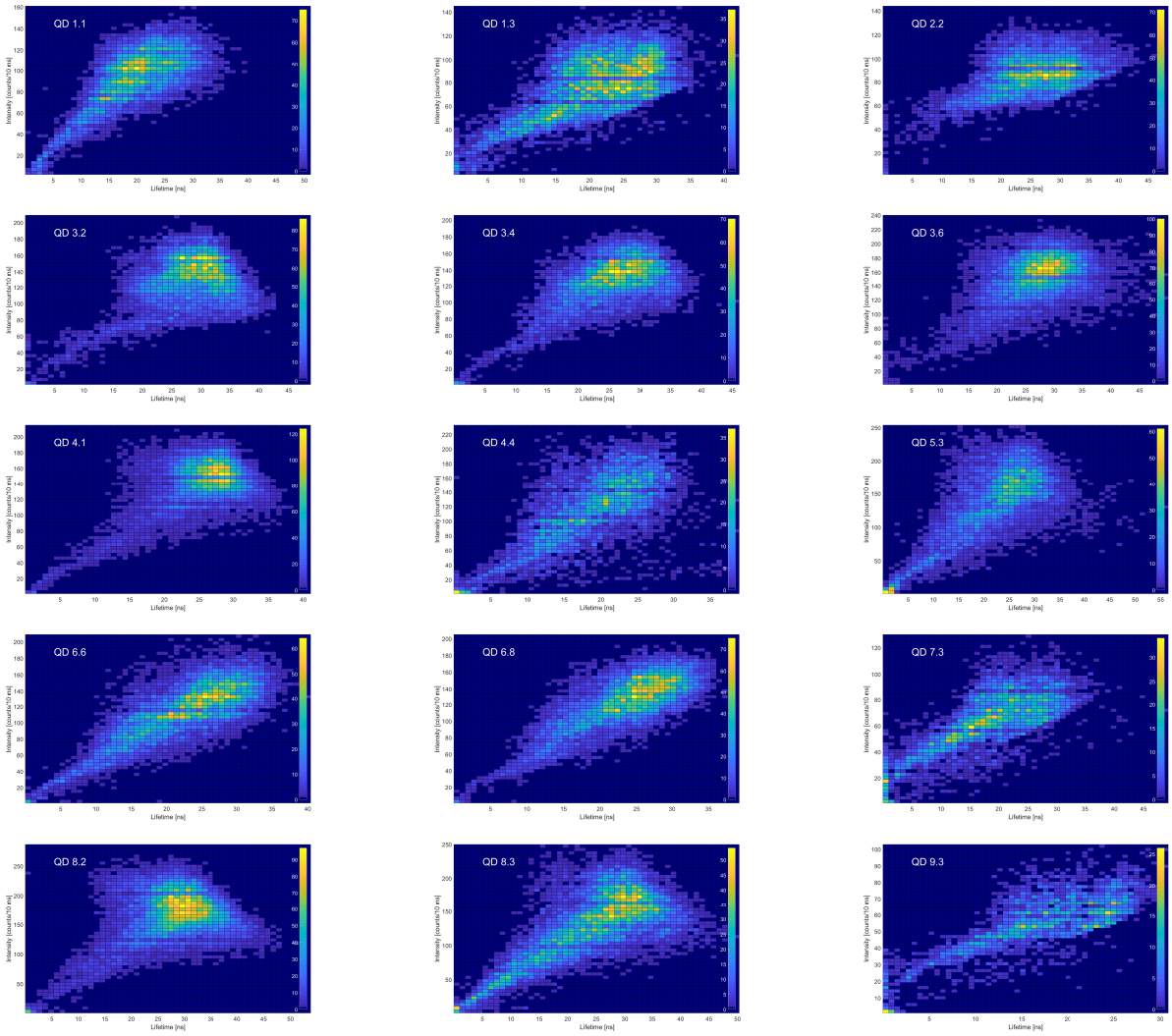

Figure S1: Fluorescence lifetime - intensity distributions (FLID) for the set of experiments with CdSeS/ZnS single quantum dots

Supplementary note 2: The second order cross-correlation function

In the experiment the Henbury-Brown-Twiss scheme is used to obtain the second order cross-correlation function $g^{(2)}(\tau)$. In the pulse experiment the function $g^{(2)}(\tau)$ shows a sequence of peaks at times equal to the integer number times the pulse period T_r (Fig. S2). We can see that the zero peak is strongly suppressed due to anti-bunching. As such, we can conclude that a single QD emission is observed.

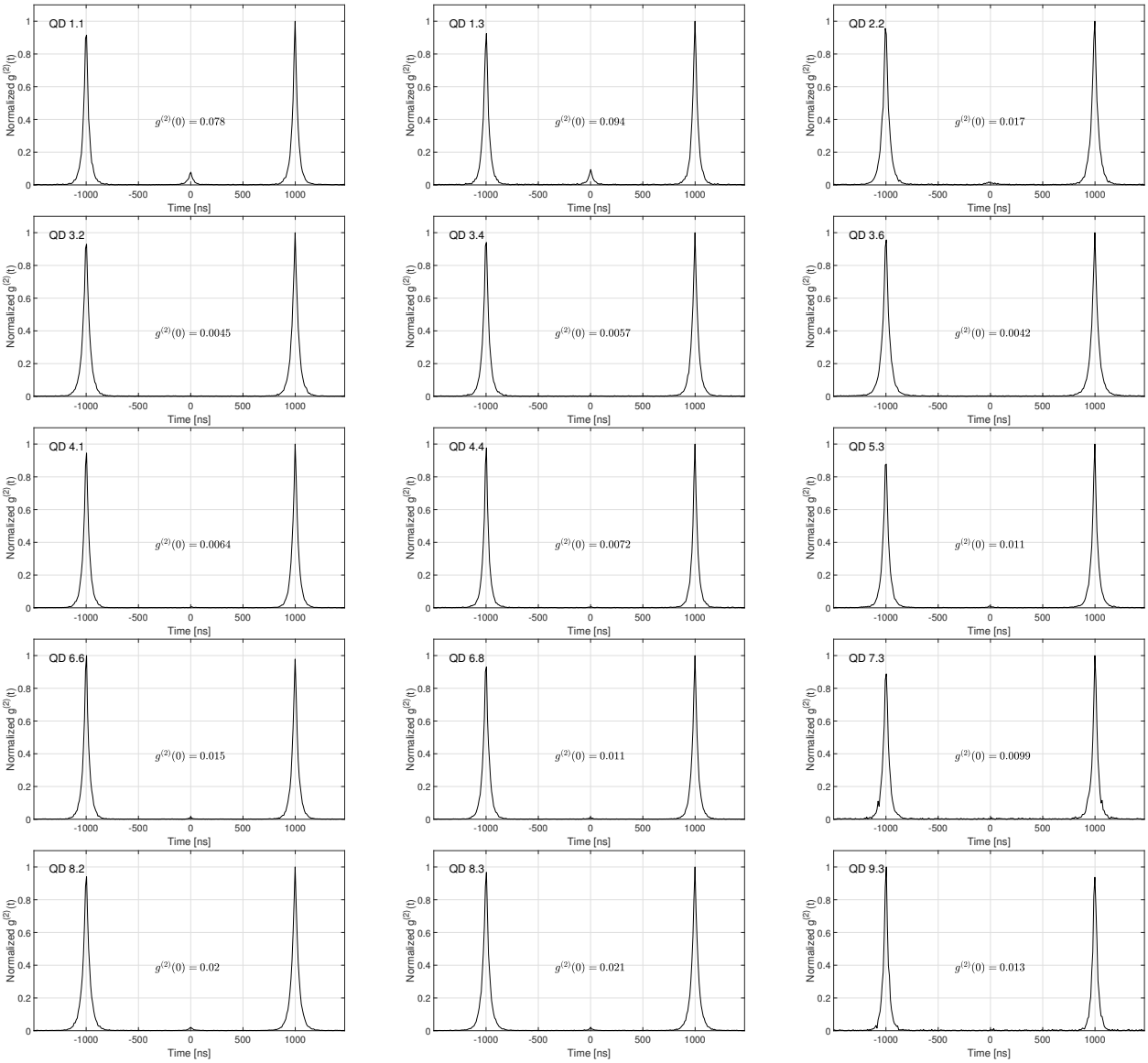

Figure S2: Short time cross-correlation function's time dependence obtained from experiments performed on the Henbury-Brown-Twiss scheme for a one pulse delay. Plots normalized by the maximum value of cross-correlation function

Supplementary note 3: Emission intensity correlation function

The averaged value of $g^{(2)}(\tau)$ at times $\tau = nT_r$, where n is an integer, is estimated as:

$$g^{(2)}(nT_r) = \frac{T}{N_1 N_2} \frac{N_{12}(nT_r)}{T_r} \tag{15}$$

where N_1 and N_2 are the total numbers of photons detected by the first and second detector, respectively, T is the time length of the detection signal, and N_{12} is the number of pairs of photons having the detection time gap within the interval from $nT_r - \delta$ to $nT_r + \delta$ where δ is much longer than the PL lifetime and much shorter than T_r. From Eq. (2) it follows that the mean number of the photons detected by the first detector and second detector after the excitation pulse at time t are:

$$N_p^1(t) = N_p^2(t) = \frac{1}{2}\alpha Y(t) N_a \tag{16}$$

It follows that:

$$\bar{N}_1 = \bar{N}_2 = \frac{T}{2T_r}\alpha \langle Y(t) \rangle N_a \tag{17}$$

and

$$\bar{N}_{12}(nT_r) = \frac{T}{4T_r}\alpha^2 \langle Y(t) Y(t + nT_r) \rangle N_a^2 \quad \text{, for } n > 0 \tag{18}$$

where $\langle \dots \rangle$ is the time average:

$$\langle A(t) \rangle = \frac{1}{T} \int_0^T A(t)\, dt \tag{19}$$

and T is the time of the measurement. Thus, the mean value of $g^{(2)}$ is:

$$\bar{g}^{(2)}(nT_r) = \frac{\langle Y(t) Y(t + nT_r) \rangle}{\langle Y(t) \rangle^2} \tag{20}$$

The two-photon correlation function (15) can be used to estimate the emission intensity autocorrelation function (ACF) defined as:

$$r(\tau) = \frac{\langle Y(t)Y(t+\tau)\rangle}{\langle Y(t)\rangle^2} - 1 = K^{(2)}(\tau) - 1 \tag{21}$$

The estimator of $K^{(2)}(\tau)$ at times $\tau = nT_r$ is:

$$\hat{K}^{(2)}(nT_r) = \frac{T}{N_1 N_2}\frac{N_{12}(nT_r)}{T_r} \tag{22}$$

When τ is much longer than T_r the value is averaged over a longer bin in order to minimize the error.

$$\hat{K}^{(2)}(nT_r) = \frac{T}{N_1 N_2}\frac{N_{12}^m(nT_r)}{mT_r} \tag{23}$$

where

$$N_{12}^m(nT_r) = \sum_{l=n-m+1}^{n} N_{12}(lT_r) \tag{24}$$

and

$$\hat{r}(nT_r) = \frac{T}{N_1 N_2}\frac{N_{12}^m(nT_r)}{mT_r} - 1 \tag{25}$$

The minimal τ is chosen as $1.6 \cdot 10^{-5}s$ with the same bin size. For a larger τ the bin value is chosen to be in the interval 0.2τ - 0.3τ.

Due to the finite times in such experiments, a strong shot noise is observed at short timescales. This noise variance can be estimated, along with the confidence interval, operating on the fact that the N_{12}^m distribution is Poisson.[3] Then N_{12}^m can be used to calculate the following variance estimation:

$$\sigma_N(nT_r) = \sqrt{N_{12}^m(nT_r)} \tag{26}$$

which can be recalculated to the $\hat{r}$ variance:

$$\sigma_r(nT_r) = \sigma_K(nT_r) = \frac{T\sigma_N(nT_r)}{mT_rN_1N_2} \tag{27}$$

A 50 Hz frequency harmonic external signal has been observed in the experimental autocorrelation function. This signal, with a manually adjusted amplitude and phase, was subtracted from the ACF to eliminate its influence. The elimination of the harmonic signal is indicated by the disappearance of the oscillations' peak within the process spectral power density.

The confidence interval for the autocorrelation function estimator (23) can be found using a 95%-confidence interval for the Poisson distribution:

$$\frac{\chi^2_{2N_{12}^m}(0.025)}{2mT_rN_1N_2}T < K^{(2)}(nT_r) < \frac{\chi^2_{2N_{12}^m+2}(0.975)}{2mT_rN_1N_2}T \tag{28}$$

where $\chi^2_\nu(\alpha)$ is the chi-squared distribution quantile, ν is the degrees of freedom number, and α is the quantile level.

The autocorrelation function $r(\tau)$ at zero time is estimated using the first peak in the two-photon correlation function. We assume that $\hat{r}(0) \approx \hat{r}(T_r)$, the value of which can be estimated by Eq.(22)

$$\hat{r}(0) = \frac{T}{N_1N_2}\frac{N_{12}(T_r)}{T_r} - 1 \tag{29}$$

Similar to Eqs.(26-27) the variance of $\hat{r}(0)$ is

$$\sigma_r(0) = \frac{T\sqrt{N_{12}(T_r)}}{T_rN_1N_2} \tag{30}$$

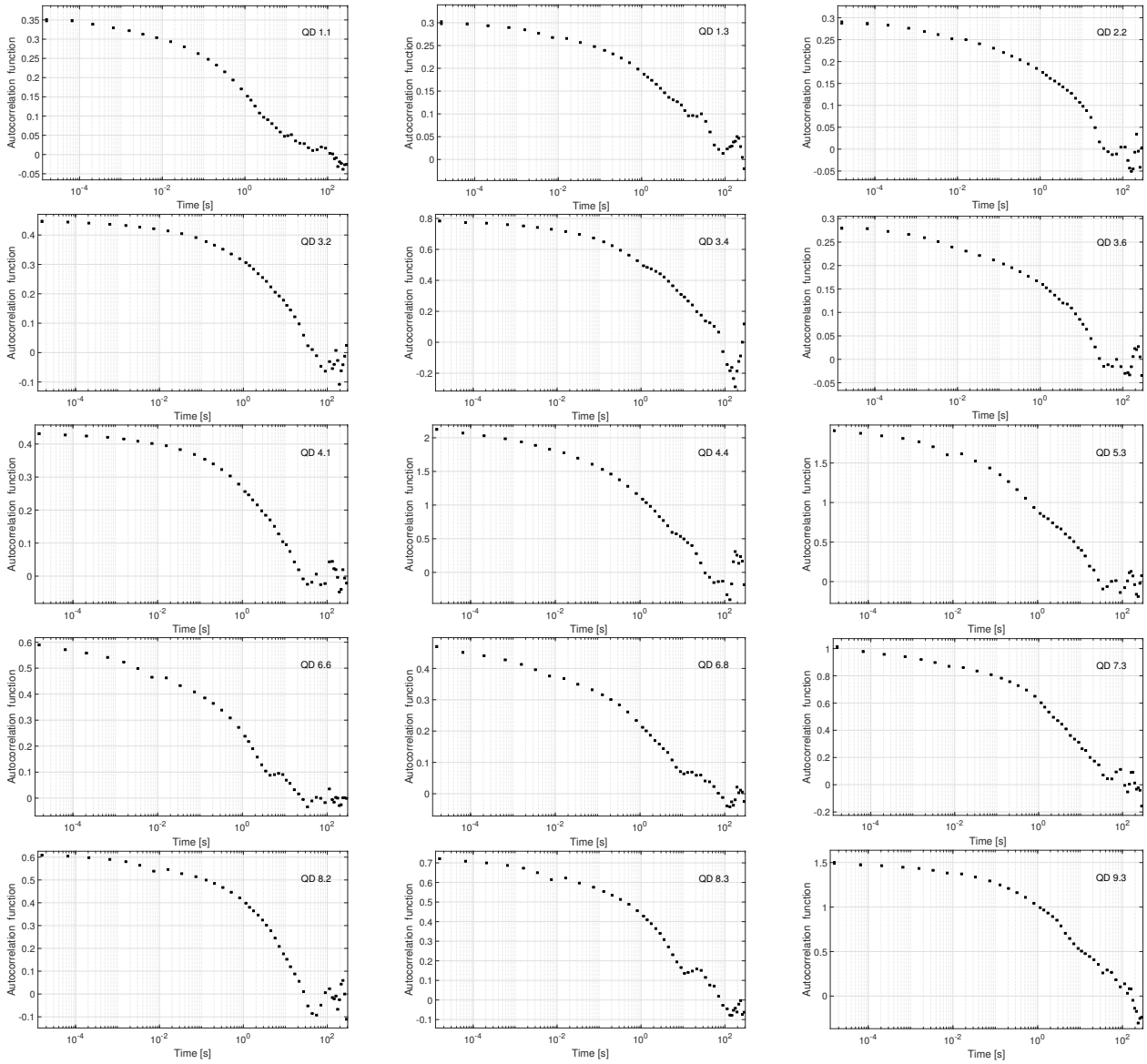

Figure S3: Experimental autocorrelation functions $r(t_n)$ with a 95%-confidence interval for the set of experiments with CdSeS/ZnS single quantum dots

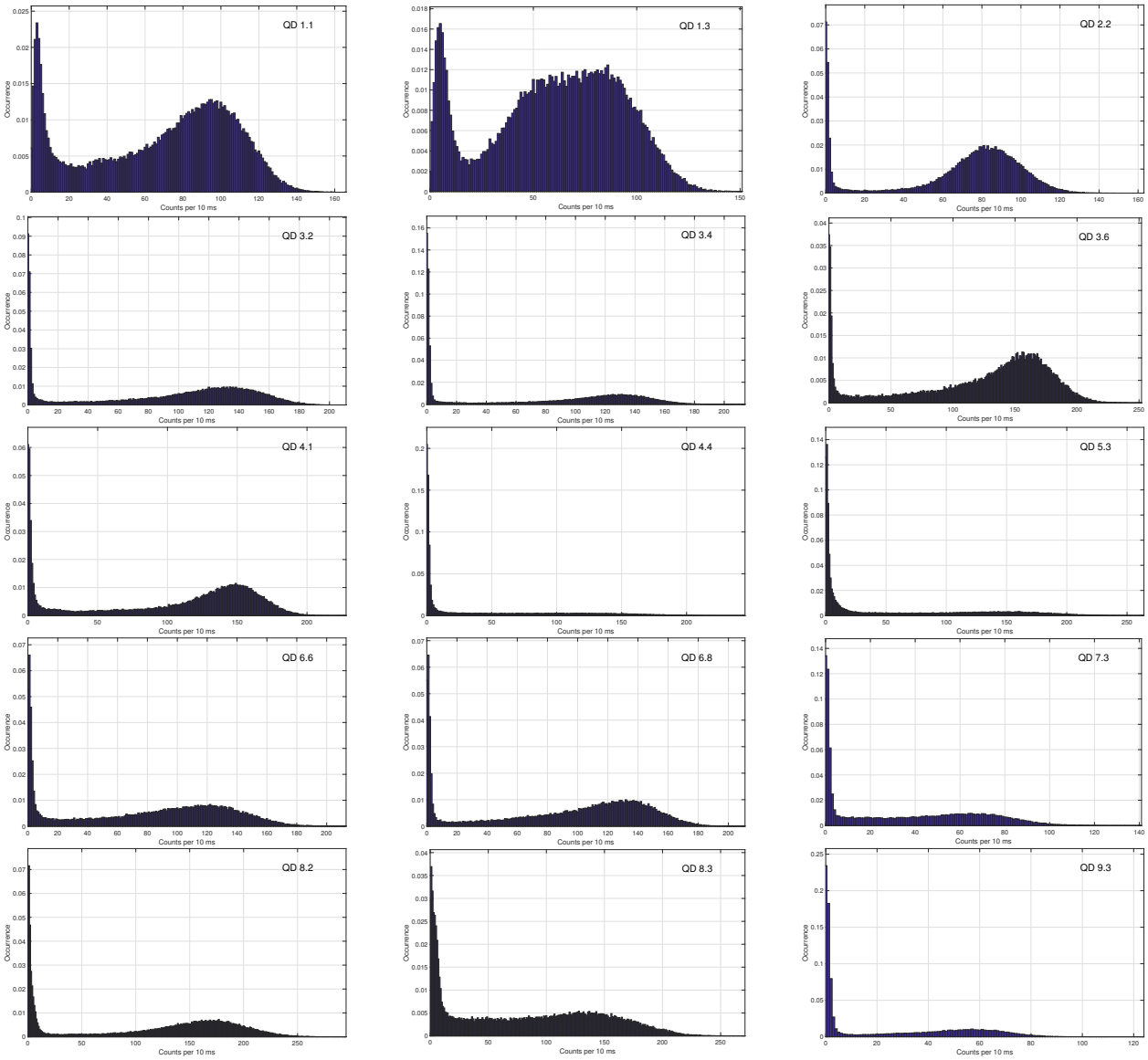

Figure S4: Photon distribution function histograms for the set of experiments with CdSeS/ZnS single quantum dots

Supplementary note 4: Estimation of the power spectral density (PSD) and its confidence interval

The random process power spectral density estimation proves to be a complicated problem. Both the signal periodogram and the autocorrelation function fast Fourier transform are shown to provide an estimate with a variance equal to the estimated value itself. [4,5]

Different power spectral density estimation methods have been proposed to solve this problem. All such methods are divided into two large groups - parametric and non-parametric. Since modern experimental techniques allow us to determine the correlation function with a higher time resolution than the blinking signal, it would be reasonable to work with a non-parametric technique that uses the autocorrelation function weighted Fourier transformation. This method is the so-called Blackman-Tukey method. [6]

To determine the power spectral density in this work, we propose to use the self-modified Blackman-Tukey method based on the interpolated autocorrelation function multiplied by the window function Fourier transform. For our data, the autocorrelation function is a set of several tens of points occupying a large area in time on unevenly distributed bins. The Blackman-Tukey method requires uniformly distributed time binning to apply the Fourier transform. The following expression can be used to get the signal PSD estimation at the chosen frequency for uniform binning: [4]

$$\hat{S}(f) = 2\Delta_t \left[r_0 + 2\sum_{n=1}^{M/2} r_n w_n \cos(2\pi f n \Delta_t) \right] ;\ 0 \leq f \leq \frac{1}{2\Delta_t} \tag{31}$$

where $\hat{S}(f)$ is the power spectral density estimation value at chosen frequency f, Δ_t is the uniform sampling bin size, r_0 is the autocorrelation sequence value at zero time, r_n is the autocorrelation sequence value within the bin number n, w_n is the window function with M bins width.

For each frequency we have chosen a characteristic time equal to the corresponding

oscillations period, so $T_f = f^{-1}$. Then we have selected a window corresponding to this frequency so that its width equals twenty corresponding periods. In addition, we have set the step $\Delta_t = T_f/100$, with which we have interpolated the correlation function within the window half-width $M/2$ to get equidistant time intervals. Such values choice guarantees us a relatively low bias and a suitable variance.

We have chosen the Blackman-Nuttall as the window function, because of its narrow peak, the continuous derivative at the edge, and the low side-lobe level:[7]

$$w_n = a_0 - a_1 \cos\left(\frac{2\pi n}{M} + \pi\right) + a_2 \cos\left(\frac{4\pi n}{M}\right) - a_3 \cos\left(\frac{6\pi n}{M} + \pi\right), \, n \leq \frac{M}{2} \tag{32}$$

where $a_0 = 0.3635819$, $a_1 = 0.4891775$, $a_2 = 0.1365995$ and $a_3 = 0.0106411$.

It can be proven that an estimation made by the Blackman-Tukey method obeys the chi-squared distribution for the value $\nu\hat{S}/S$ (S is actual PSD), where ν is the degrees of freedom number, defined as:[4,5]

$$\nu \equiv \frac{2\hat{S}^2}{\sigma_S^2} \tag{33}$$

where σ_S^2 stands for the variance of $\hat{S}(f)$

For a well-defined correlation function without shot noise, ν is estimated through the following expression:

$$\nu = \frac{2T/\Delta_t}{\sum w_n^2} \tag{34}$$

In the presence's case of additional errors associated with shot noise, an additional variance appears:

$$\sigma_{\mathcal{N}}^2 = [2\Delta_t]^2 \left[\sigma_{r_0}^2 + 2\sum_{n=1}^{M/2} \sigma_{r_n}^2 w_n^2 \cos(2\pi f n \Delta_t)^2\right] \tag{35}$$

where σ_{r_n} is the variance at a given bin n, estimated the same way we did in expression

(27), but for interpolated bins. The probability distribution of these errors is believed to be normal.

In this case, the final variance is the sum of variances if the sources of errors are considered to be independent:

$$\sigma_S^2 = \sigma_{\mathcal{N}}^2 + \sigma_{\chi^2}^2 \tag{36}$$

where

$$\sigma_{\chi^2}^2 = \frac{\hat{S}^2 \sum w_n^2 \Delta_t}{T} \tag{37}$$

For $\nu < 100$ (takes place at low frequencies), the error associated with the shot noise is negligible, and the 95%-confidence interval can be calculated using the chi-squared distribution:

$$\frac{\nu \hat{S}}{\chi_\nu^2(0.975)} < S < \frac{\nu \hat{S}}{\chi_\nu^2(0.025)} \tag{38}$$

where $\chi_\nu^2(\alpha)$ is the chi-squared distribution quantile.

For $\nu > 100$, the chi-squared distribution can be considered as normal due to the chi-squared asymptotics. At this step, both errors can be included in one expression (36), which is equivalent to the two normal distributions convolution, and one can use the sum variance to calculate the 95%-confidence interval:

$$\hat{S} - 1.96 \cdot \sigma_S < S < \hat{S} + 1.96 \cdot \sigma_S \tag{39}$$

It is clear that shot noise errors have a dominant contribution at high frequencies.

The estimation results are presented in Fig. S5

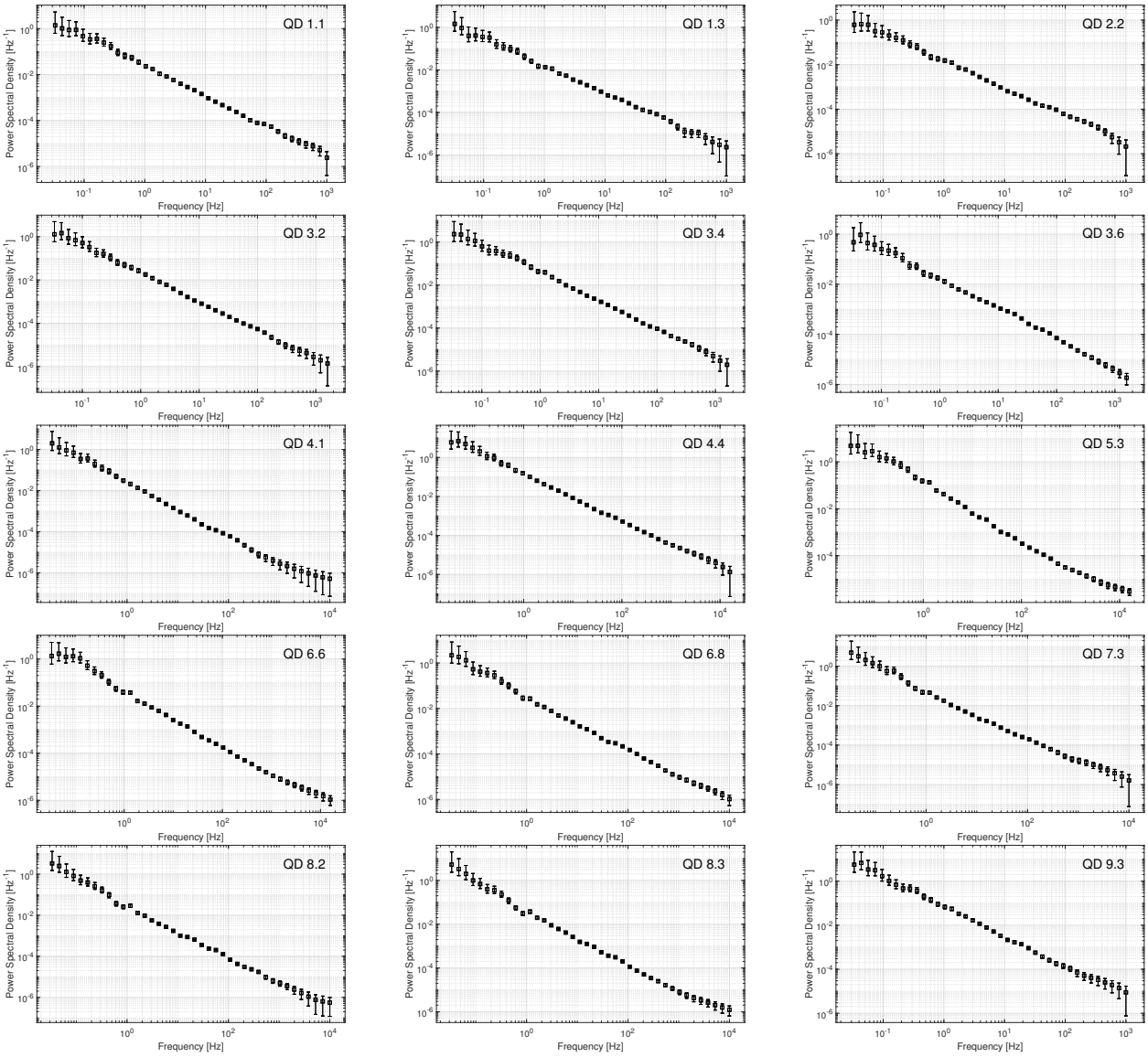

Figure S5: Power spectral densities of single quantum dots luminescence blinking obtained by the modified Blackman-Tukey method

Supplementary note 5: PSD estimation frequency range

The maximum resolved frequency is ideally determined by the smallest available time in the autocorrelation function, which in our case is $1.6 \cdot 10^{-5}$ s. The frequency of $3.1 \cdot 10^{4}$ Hz corresponds to this time. Unfortunately, there are additional restrictions present in an experiment.

For an ACF with some uncorrelated noise fluctuations, which become more intense with shorter times, its Fourier transform contains the errors associated with those fluctuations (see (35)), which value increases with frequency. For any given PSD we have chosen the point at which the effect of such errors becomes comparable with the value of the estimated power density, so that point is the highest frequency bound point of the PSD.

Thus, for each trajectory, this point changes and lies within the range from 10^{3} Hz to $1.5 \cdot 10^{4}$ Hz, which is close to maximal resolved frequency in an ideal situation.

The minimum resolvable frequency is determined by the maximum window width, i.e. there cannot be a window width longer then the maximal time of the autocorrelation function $T_A = 300$ s. In our consideration we have chosen the window parameters so that:

$$f_{\min} = \frac{10}{T_A} \tag{40}$$

Thus, in our investigation the lower frequency is bound at around about $3.3 \cdot 10^{-2}$ Hz.

The frequency range chosen was divided into 40 logarithmically equidistant points at which the power spectral density was estimated.

Supplementary note 6: Estimation of the minimal PLQY within the MRC model

The PLQY of the QD emission within the MRC model[2,8] can be expressed as

$$Y(t) = \frac{k_r}{k_r + k_t(t)} \tag{41}$$

where k_r is the radiative recombination rate. The total trapping reaction rate within this model is a sum of the trapping rates for each RC.

$$k_t(t) = \sum_{i=1}^{N} k_i \sigma_i(t) + k_b. \tag{42}$$

where k_i is the trapping rate for the i-th TLS, k_b is the background rate. Each stochastic variable $\sigma_i(t)$ randomly jumps between two values - 0 and 1.

The maximal emission intensity corresponds to the configuration of the TLS when all σ_i are equal to 0. It follows from Eqs. (42) and (41) that the PLQY of this configuration is $PLQY = k_r/(k_r + k_b)$. Usually, the PLQY in the ON state is close to 100%, so we can set $k_0 \ll k_r$. The jump of the single i-th TLS changes the quantum yield to the value $k_r/(k_r+k_i+k_b)$. If $k_i \gg k_r$ one jump will cause a huge decrease of the intensity. This behavior is very different from the nearly continuous intensity distribution seen in the experiment. In order to reproduce that, one should set k_i values to be close to k_r. Thus the lowest photoluminescence quantum yield corresponding to the configuration when all σ_i are equal 1, value Eq. (41), has to be in the order of $1/(N + 1)$. To make the minimal PLQY value close to 1% one has to assume that the number N of the quasi-stationary defects on the QD surface is around 100 which is very unlikely.

Supplementary note 7: Electron-phonon coupling value dependence of the trapping rate

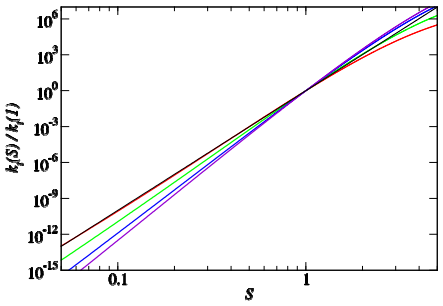

Figure S6: The trapping rate dependence on the Huang-Rhys parameter S at T=300 K (red line), T=200 K (green line), T=100 K (blue line) and T= 50 K(violet line). The thin black line represents S^{10}. The rest of the parameters are $\Delta E = -355$ meV, $\lambda_c = 10$ meV, $\hbar\omega_{LO} = 26$ meV

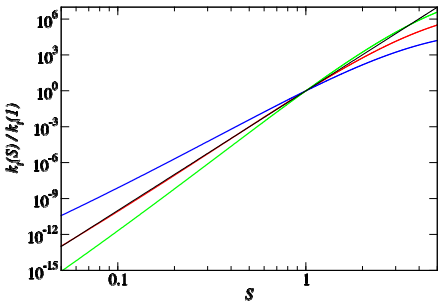

Figure S7: The trapping rate dependence on the Huang-Rhys parameter S at $\Delta E = -300$ meV (blue line), $\Delta E = -355$ meV (red line) and $\Delta E = -400$ meV K (green line). The thin black line represents S^{10}. The rest of the parameters are $T = 300$ K, $\lambda_c = 10$ meV, $\hbar\omega_{LO} = 26$ meV

The rate of the hole trapping process assisted by multiple optical phonon excitations can be expressed by the well known Marcus-Jortner formula (for example[9])

$$k_t = \frac{V^2}{\hbar}\sqrt{\frac{\pi}{\lambda_c k_B T}}\sum_{n=-\infty}^{\infty} P_n \exp\left(-\frac{(\Delta E + \lambda_c + n\hbar\omega_{LO})^2}{4\lambda_c k_B T}\right) \tag{43}$$

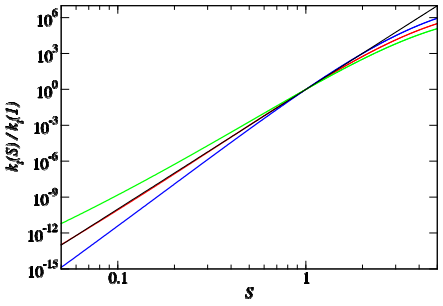

Figure S8: The trapping rate dependence on the Huang-Rhys parameter S at $\lambda_c = 5$ meV (blue line), $\lambda_c = 10$ meV (red line) and $\lambda_c = 15$ meV (green line). The thin black line represents S^{10}. The rest of the parameters are $T = 300$ K, $\Delta E = -355$ meV, $\hbar\omega_{LO} = 26$ meV

where V is the electron exchange matrix element, T is the temperature, λ_c is the reorganization energy of the classical modes, ω_{LO} is the frequency of the optical longitudinal phonons and ΔE is the difference between the QD's electronic energy of the state with the trapped hole and the energy of the excited state, P_n is the probability of exciting n phonon quanta during the transition

$$P_n = I_n\left(\frac{S}{\sinh\tilde{\omega}}\right)\exp\left(n\tilde{\omega} - S\coth\tilde{\omega}\right) \tag{44}$$

where $I_n(z)$ is the modified Bessel function, $\tilde{\omega} = \hbar\omega_{LO}/(2k_BT)$ and S is the Huang-Rhys parameter $S = \lambda/(\hbar\omega_{LO})$ determined by the reorganization energy λ, characterizing the interaction between the electronic system and optical longitudinal phonons. When ΔE is negative and its modulus is much greater than λ_c and $\hbar\omega_{LO}$ then a major contribution to the sum in Eq.(43) comes from the terms with value n around $|\Delta E|/(\hbar\omega_{LO})$. As a result the dependence of the trapping rate Eq.(43) on S when $S < 1$ can be approximated by a power law, as seen from the numeric calculations results presented on Fig. S1-S3.

$$k_t(S) = k_0 S^{\alpha} \tag{45}$$

The exponent α weakly depends on the temperature (Fig. S6), ΔE (Fig. S7) and λ_c (Fig.

S8): Choosing the parameters $\Delta E = -355$ meV, $T = 300$ K, $\lambda_c = 10$ meV, $\hbar\omega_{LO} = 26$ meV, we set $\alpha = 10$.

Supplementary note 8: PSD for an isolated two-level system (TLS)

Let us suppose that the single QD is described by an isolated stochastic two-level system. There are two configurations of the system, corresponding to $\sigma = 0$ and $\sigma = 1$. The dynamics of the system obey the following master equation in matrix form:[10]

$$\frac{\mathrm{d}}{\mathrm{d}t}\vec{\boldsymbol{p}}(t) = \hat{\boldsymbol{w}}\vec{\boldsymbol{p}}(t) \tag{46}$$

The vector of probabilities $\vec{\boldsymbol{p}}(t)$ is defined as:

$$\vec{\boldsymbol{p}}(t) \equiv \begin{pmatrix} p_0(t) \\ p_1(t) \end{pmatrix} \tag{47}$$

where $p_0(t)$, $p_1(t)$ are the probabilities of the system to be in the 0 and 1 configuration at time t, correspondingly.

The matrix $\hat{\boldsymbol{w}}$ is defined as:

$$\hat{\boldsymbol{w}} \equiv \begin{pmatrix} -\gamma^+; & \gamma^- \\ \gamma^+; & -\gamma^- \end{pmatrix} \tag{48}$$

where γ^+ is the rate of 0 to 1 transition and γ^- is the rate of 1 to 0 transition. We also define the general switching rate $\Gamma = \gamma^+ + \gamma^-$ and the stationary probability p to be in 1 configuration.

$$\gamma^+ = \Gamma p$$

$$\gamma^- = \Gamma(1-p)$$

The vector $\vec{\boldsymbol{p}}$ obeys the normalization condition:

$$p_0(t) + p_1(t) = 1 \tag{49}$$

The stationary solution for equation (46) has the following form:

$$\vec{\boldsymbol{p}}^{st} = \begin{pmatrix} \frac{\gamma^-}{\Gamma} \\ \frac{\gamma^+}{\Gamma} \end{pmatrix} \equiv \begin{pmatrix} 1-p \\ p \end{pmatrix} \tag{50}$$

The eigenvalues and eigenvectors of the matrix $\hat{\boldsymbol{w}}$ can be found using the following set of equations:

$$\hat{\boldsymbol{w}}\vec{\boldsymbol{p}}_\lambda^{\text{right}} = \lambda\vec{\boldsymbol{p}}_\lambda^{\text{right}} \tag{51}$$

$$\left(\vec{\boldsymbol{p}}_\lambda^{\text{left}}\right)^T \hat{\boldsymbol{w}} = \lambda \left(\vec{\boldsymbol{p}}_\lambda^{\text{left}}\right)^T \tag{52}$$

where symbol T stands for transposition. This leads to the following eigenvalues equation:

$$\det\left(\hat{\boldsymbol{w}} - \lambda\hat{\boldsymbol{I}}\right) = 0 \tag{53}$$

where $\hat{\boldsymbol{I}}$ is the identity matrix.

The obvious solutions for eigenvalues are:

$$\lambda_{1,2} = 0; -\Gamma; \tag{54}$$

It turns out to be convenient to use the following diagonalization matrices comprising the right and left eigenvectors:

$$\hat{\boldsymbol{w}} = \hat{\boldsymbol{v}}^{\text{right}}\hat{\boldsymbol{d}}\hat{\boldsymbol{v}}^{\text{left}} \tag{55}$$

where

$$\hat{\boldsymbol{d}} = \begin{pmatrix} 0 & 0 \\ 0 & -\Gamma \end{pmatrix} \tag{56}$$

and

$$\hat{\boldsymbol{v}}^{\text{right}} = \begin{pmatrix} 1-p; & -1; \\ p; & 1; \end{pmatrix} \equiv \left(\vec{\boldsymbol{p}}^{\text{right}}_{\lambda=0}; \quad \vec{\boldsymbol{p}}^{\text{right}}_{\lambda=-\Gamma}; \right) \tag{57}$$

$$\hat{\boldsymbol{v}}^{\text{left}} = \begin{pmatrix} 1; & 1; \\ -p; & 1-p; \end{pmatrix} \equiv \begin{pmatrix} \left(\vec{\boldsymbol{p}}^{\text{left}}_{\lambda=0}\right)^T \\ \left(\vec{\boldsymbol{p}}^{\text{left}}_{\lambda=-\Gamma}\right)^T \end{pmatrix} \tag{58}$$

The formal solution of the Eq. (46) is:

$$\vec{\boldsymbol{p}}(t) = \exp\left(\hat{\boldsymbol{w}}t\right)\vec{\boldsymbol{p}}(0) \equiv \hat{\boldsymbol{G}}(t)\vec{\boldsymbol{p}}(0) \tag{59}$$

Within the Markov stochastic processes theory the quantum yield autocorrelation function (21) can be expressed as:

$$r(t) = \frac{1}{\langle Y \rangle^2} \sum_{\sigma=0}^{1} \sum_{\sigma'=0}^{1} Y_\sigma Y_{\sigma'} G_{\sigma\sigma'}(t) p^{st}_{\sigma'} - 1 \tag{60}$$

where Y_0 and Y_1 are the PL quantum yield of the configuration 0 and 1, respectively.

The quantum yield mean value is:

$$\langle Y \rangle = \sum_{\sigma=0}^{1} Y_\sigma p^{st}_\sigma \tag{61}$$

The matrix exponent can be expressed as:

$$\hat{\boldsymbol{G}}(t) = \hat{\boldsymbol{v}}^{\text{right}} \exp\left(\hat{\boldsymbol{d}}t\right) \hat{\boldsymbol{v}}^{\text{left}} \tag{62}$$

Applying this expression to Eq. (60) we get the following expression for the intensity autocorrelation function:

$$r(t) = \frac{\gamma^- \gamma^+}{\Gamma^2} \frac{(Y_1 - Y_0)^2}{\langle Y \rangle^2} e^{-\Gamma t} \tag{63}$$

In this case, the theoretical power spectral density can be obtained using the Wiener -

Khinchin theorem. The PSD turns out to be the Lorentzian function:

$$S(f) = 4\int_0^\infty r(t)\cos(2\pi f t)\,\mathrm{d}t = \frac{4\gamma^-\gamma^+}{\Gamma}\frac{(Y_1 - Y_0)^2}{\langle Y\rangle^2}\frac{1}{\Gamma^2 + (2\pi f)^2};\ 0 \le f < \infty \tag{64}$$

Supplementary note 9: PSD for set of uncorrelated two-level systems

Our model of QD blinking includes N uncorrelated TLS. The configuration of i-th TLS is described by the index σ_i. The switching rates of this TLS are γ_j^+ and γ_j^i. Each of the 2^N configurations of the system is described by the index:

$$\Sigma = \{\sigma_N, \ldots, \sigma_1\} \tag{65}$$

The master equation of the system has the following form:[10]

$$\frac{\mathrm{d}}{\mathrm{d}t}\vec{\boldsymbol{P}}(t) = \hat{\boldsymbol{W}}\vec{\boldsymbol{P}}(t) \tag{66}$$

where each element $P_\Sigma(t)$ of the vector $\vec{\boldsymbol{P}}(t)$ is the probability to be in the configuration Σ at time t. The matrix $\hat{\boldsymbol{W}}$ has the following nonzero elements for each Σ and i:

$$W_{\Sigma\Sigma} = -\sum_{j=1}^{N}\gamma_j^{\sigma_j}$$

$$W_{\Sigma\Sigma^i} = \gamma_i^{\bar{\sigma}_i} \tag{67}$$

where Σ^i is:

$$\Sigma^i = \{\sigma_N, \ldots, \overline{\sigma}_i, \ldots, \sigma_1\} \tag{68}$$

The symbol $\overline{\sigma}_i$ means negation, and $\gamma_j^{\sigma_j} = \gamma_j^-$, if $\sigma_j = 1$ and γ_j^+, if $\sigma_j = 0$. All other

elements of matrix $\hat{\boldsymbol{W}}$ are equal to zero. The matrix $\hat{\boldsymbol{W}}$ can be written in the other form:

$$\hat{\boldsymbol{W}} = \bigoplus_{i=1}^{N} \hat{\boldsymbol{w}}_i \tag{69}$$

where $\bigoplus$ stands for Kronecker summation.

The steady-state is defined as:

$$\hat{\boldsymbol{W}} \vec{\boldsymbol{P}}^{st} = 0 \tag{70}$$

The normalization condition for the master equation is:

$$\sum_{\Sigma} P_{\Sigma} = 1 \tag{71}$$

The formal system solution is:

$$\vec{\boldsymbol{P}}(t) = \exp\left(\hat{\boldsymbol{W}} t\right) \vec{\boldsymbol{P}}_0 \equiv \hat{\boldsymbol{G}}(\boldsymbol{t}) \vec{\boldsymbol{P}}_0 \tag{72}$$

The stationary Markovian process quantum yield autocorrelation function is:

$$r(t) = \frac{1}{\langle Y \rangle^2} \sum_{\Sigma\Sigma'} Y_{\Sigma} Y_{\Sigma'} G_{\Sigma\Sigma'}(t) P_{\Sigma'}^{st} - 1 \tag{73}$$

where Y_{Σ} is the quantum yield of the configuration Σ. Applying Eqs. (12) and (45) and Eq. (5) from the main text we have:

$$Y_{\Sigma} = \frac{k_r}{k_r + k_t(\Sigma)} \tag{74}$$

where

$$k_t(\Sigma) = k_0 S_{\Sigma}^{\alpha} \tag{75}$$

and $S_{\Sigma} = s_0 + \sum_{i=1}^{N} \sigma_i s_i$.

Introducing the diagonal matrix $\hat{\boldsymbol{Y}}$, so that $\hat{Y}_{\Sigma\Sigma} = Y_{\Sigma}$ and the dot product according to

the following rule:

$$\left(\vec{\boldsymbol{X}}, \vec{\boldsymbol{Y}}\right) \equiv \sum_{\Sigma} X_{\Sigma} Y_{\Sigma} \tag{76}$$

one can rewrite the expression for autocorrelation function into a more compact form:

$$r(t) = \frac{1}{\langle Y \rangle^2} \left(\vec{\boldsymbol{Y}}, \hat{\boldsymbol{G}}(t)\hat{\boldsymbol{Y}}\vec{\boldsymbol{P}}^{\boldsymbol{st}}\right) - 1 \tag{77}$$

The mean value of the quantum yield is:

$$\langle Y \rangle = \left(\vec{\boldsymbol{Y}}, \vec{\boldsymbol{P}}^{st}\right) \tag{78}$$

The matrix $\hat{\boldsymbol{W}}$ can be diagonalized:

$$\hat{\boldsymbol{W}} = \hat{\boldsymbol{V}}\hat{\boldsymbol{D}}\hat{\boldsymbol{V}}^{-1} \tag{79}$$

where $\hat{\boldsymbol{D}}$ is a diagonal matrix and $\hat{\boldsymbol{V}}$ is a transition matrix. Then, the operator $\hat{\boldsymbol{G}}(t)$ can be expressed as:

$$\hat{\boldsymbol{G}}(t) = \hat{\boldsymbol{V}} \exp(\hat{\boldsymbol{D}}t)\hat{\boldsymbol{V}}^{-1} \tag{80}$$

Due to Eq. (69) the following expression for matrices $\hat{\boldsymbol{V}}$ and $\hat{\boldsymbol{V}}^{-1}$ can be used:

$$\hat{\boldsymbol{V}} = \bigotimes_{i=1}^{N} \hat{\boldsymbol{v}}_i^{\text{right}}, \tag{81}$$

$$\hat{\boldsymbol{V}}^{-1} = \bigotimes_{i=1}^{N} \hat{\boldsymbol{v}}_i^{\text{left}}, \tag{82}$$

where $\boldsymbol{v_i}^{\text{right}}$ and $\boldsymbol{v_i}^{\text{left}}$ are isolated two-level systems transition matrices, $\bigotimes$ stands for Kronecker product. In this case, $\hat{\boldsymbol{D}}$ consists of different unique isolated two-level systems eigenvalues sums. This sequence order depends on the order of the two-level systems in the used

notation. The $\vec{\boldsymbol{P}}^{st}$ can also be calculated as:

$$\vec{\boldsymbol{P}}^{\boldsymbol{st}} = \bigotimes_{i=1}^{N} \vec{\boldsymbol{p}}_i^{st} \tag{83}$$

The quantum yield power spectral density is:

$$S(f) = \frac{1}{\langle Y \rangle^2} \left(\vec{\boldsymbol{Y}}, \widetilde{\boldsymbol{G}}(f) \hat{\boldsymbol{Y}} \vec{\boldsymbol{P}}^{\boldsymbol{st}} \right) \tag{84}$$

where $\widetilde{\boldsymbol{G}}(f)$ is the $\hat{\boldsymbol{G}}(t)$ Fourier image.

$$\widetilde{\boldsymbol{G}}(f) = 4 \int_0^{\infty} \hat{\boldsymbol{G}}(t) \cos(2\pi f t)\, \mathrm{d}t = \hat{\boldsymbol{V}} \frac{4|\hat{\boldsymbol{D}}|}{(2\pi f)^2 + \hat{\boldsymbol{D}}^{\,2}} \hat{\boldsymbol{V}}^{-1};\ 0 \le f < \infty \tag{85}$$

That corresponds to the $2^N - 1$ different independent Lorentzian functions sum, the width of which is defined by a diagonal matrix $\hat{\boldsymbol{D}}$ elements.

For each of the 2^N states, the probability to detect n photons per bin Δt has the Poisson distribution:[10]

$$q_{\Sigma}(n) = \frac{\overline{N}_{\Sigma}^{\,n}}{n!} e^{-\overline{N}_{\Sigma}} \tag{86}$$

where $\overline{N}_{\Sigma}$ is the mean number of detected photons by state Σ within the time bin Δt. The total probability distribution to detect n photons per time bin size of Δt is the weighted sum of the all states distributions with corresponding steady-state probabilities:

$$Q(n) = \sum_{\Sigma} q_{\Sigma}(n) P_{\Sigma}^{st} = \left(\vec{\boldsymbol{q}}(n), \vec{\boldsymbol{P}}^{\boldsymbol{st}} \right) \tag{87}$$

From Eq. (5) we have:

$$\overline{N}_{\Sigma} = A \overline{Y}_{\Sigma} + b \tag{88}$$

where $\overline{Y}_{\Sigma}$ is defined as:

$$\overline{Y}_{\Sigma} \equiv \frac{1}{\Delta t} \int_0^{\Delta t} \sum_{\Sigma'} Y_{\Sigma'} G_{\Sigma'\Sigma}(t)\, \mathrm{d}t = \sum_{\Sigma'} Y_{\Sigma'} \overline{G}_{\Sigma'\Sigma} \tag{89}$$

where

$$\overline{\boldsymbol{G}} = \hat{\boldsymbol{V}} \frac{1}{\hat{\boldsymbol{D}}\Delta t} \left[\exp\left(\hat{\boldsymbol{D}}\Delta t\right) - 1 \right] \hat{\boldsymbol{V}}^{-1} \tag{90}$$

Supplementary note 10: Fitting procedure

To reduce the number of fitting parameters, the following reasoning about TLS switching rates Γ_i has been used. Since each TLS must be the set of two potential energy minima, the rate constant must be modified with the thermal activation exponent. Assuming the transition energies to be evenly distributed among the TLSs, it can be expected that the transition rates are evenly distributed on a logarithmic scale. Therefore, we have chosen Γ_i so that they are logarithmically evenly distributed in the investigated range. For each of the chosen QD's trajectories the boundaries were slightly changed manually to match the behavior of PSD at the boundary frequencies.

The fitting procedure obeys the standard maximum likelihood method. The negative logarithm of the likelihood function consists of 2 parts:

$$-\ln L = -\ln L_{PSD} - \ln L_Q \tag{91}$$

where L_{PSD} is a likelihood of the PSD estimator and L_Q stands for the likelihood of the photon distribution. The PSD estimator likelihood consists of the two terms:

$$-\ln L_{PSD} = -\ln L_{\chi^2} - \ln L_{\mathcal{N}} \tag{92}$$

where L_{χ^2} stands for the term coming from the chi-squared distributed part of PSD estimator and $L_{\mathcal{N}}$ - from the part that obeys normal distribution.

$$-\ln L_{\chi^2} = \sum_{f<f_\nu} \left[-\left(\frac{\nu(f)}{2} - 1\right) \ln X(f) + \frac{X(f)}{2} + \ln \Gamma\left(\frac{\nu(f)}{2}\right) + \frac{\nu(f)}{2} \ln 2 \right]; \tag{93}$$

$$-\ln L_{\mathcal{N}} = \sum_{f>f_\nu} \left[\frac{(\hat{S}(f) - S_{th}(f))^2}{2\sigma_S^2(f)} + \frac{1}{2} \ln 2\pi \right] \tag{94}$$

where $\Gamma(n)$ corresponds to Euler's gamma function, $\nu(f)$ is the chi-squared distribution degrees of the freedom number, $X(f) = \nu(f)\hat{S}(f)/S_{th}(f)$, f_ν is the frequency that corresponds to the moment when the degrees of freedom number becomes larger than 100 (at this moment a transition from chi-squared to normal distribution is assumed), $S_{th}(f)$ corresponds to the theoretical prediction (84), which depends on the model parameters s_0, s_i, p_i, k_0/k_r, b. The function L_Q corresponds to the number of detected photons distribution contribution, which must obey a multinomial distribution.

$$-\ln L_Q = -\sum_n M(n) \ln Q_{th}(n) - \ln \binom{M}{M(1), ..., M(n_{\max})} \tag{95}$$

where $M(n)$ is the number of bins with n detected photons, M is the total number of bins in the trajectory, $\binom{M}{M(1),...,M(n_{\max})}$ is the multinomial coefficient, $n_{\max}$ is the maximum photon level, and $Q_{th}(n)$ is the theoretical prediction (87) depending on the model parameters. The coefficient A was found using experimental data

$$A = \frac{\langle N \rangle - b}{\langle Y \rangle} \tag{96}$$

where $\langle N \rangle$ is the averaged number of photons among experimental distribution per time bin.

The minimum of the likelihood function negative logarithm has been found using a self-made MATLAB program. A few particular TLSs were excluded from consideration for almost every investigated trajectory during the minimization procedure. The initial number of TLSs was set to 10.

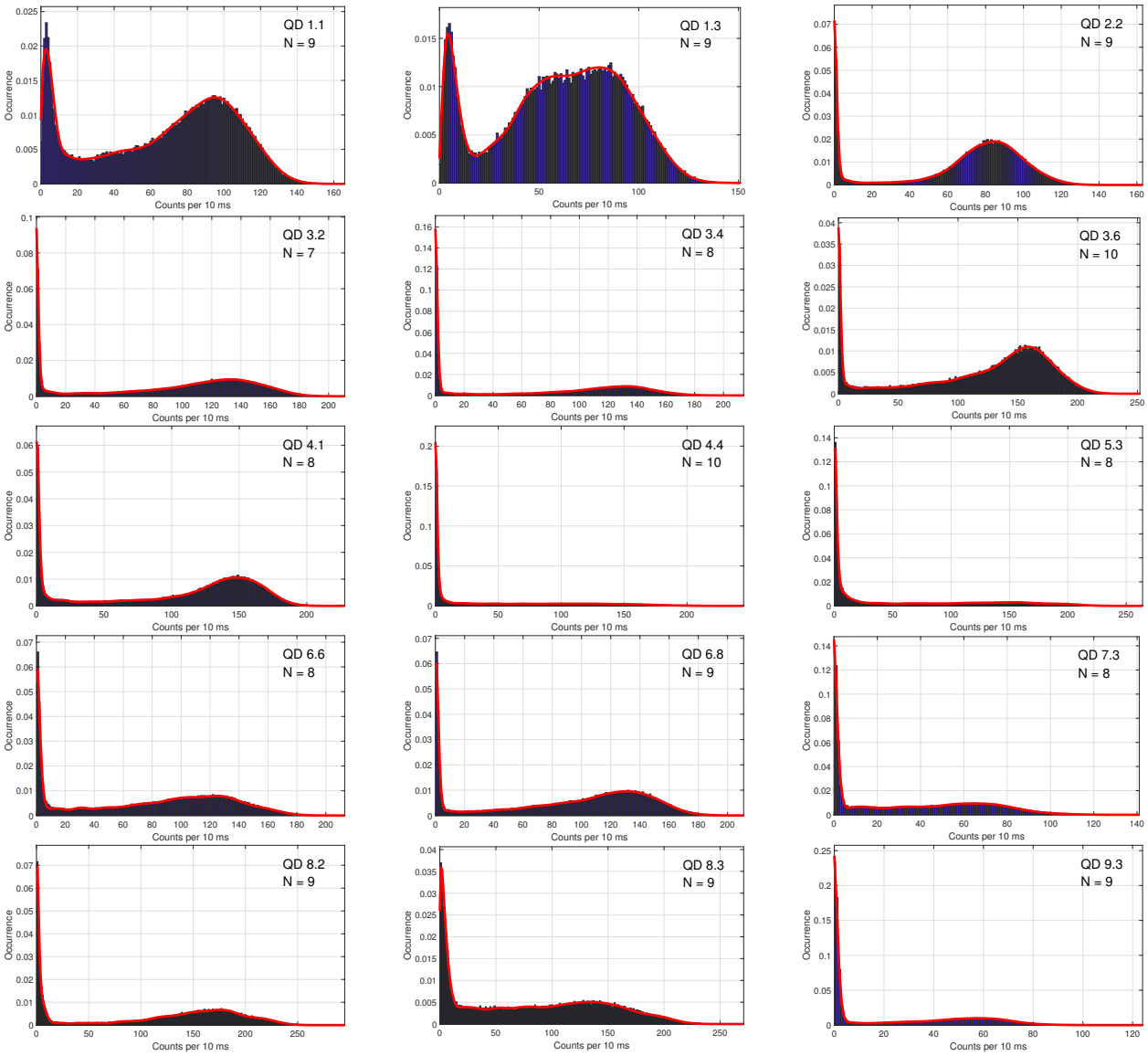

Figure S9: Experimental probability distribution of detected photon data (blue bars) model fits (red thin line) for the set of experiments with CdSeS/ZnS single quantum dots

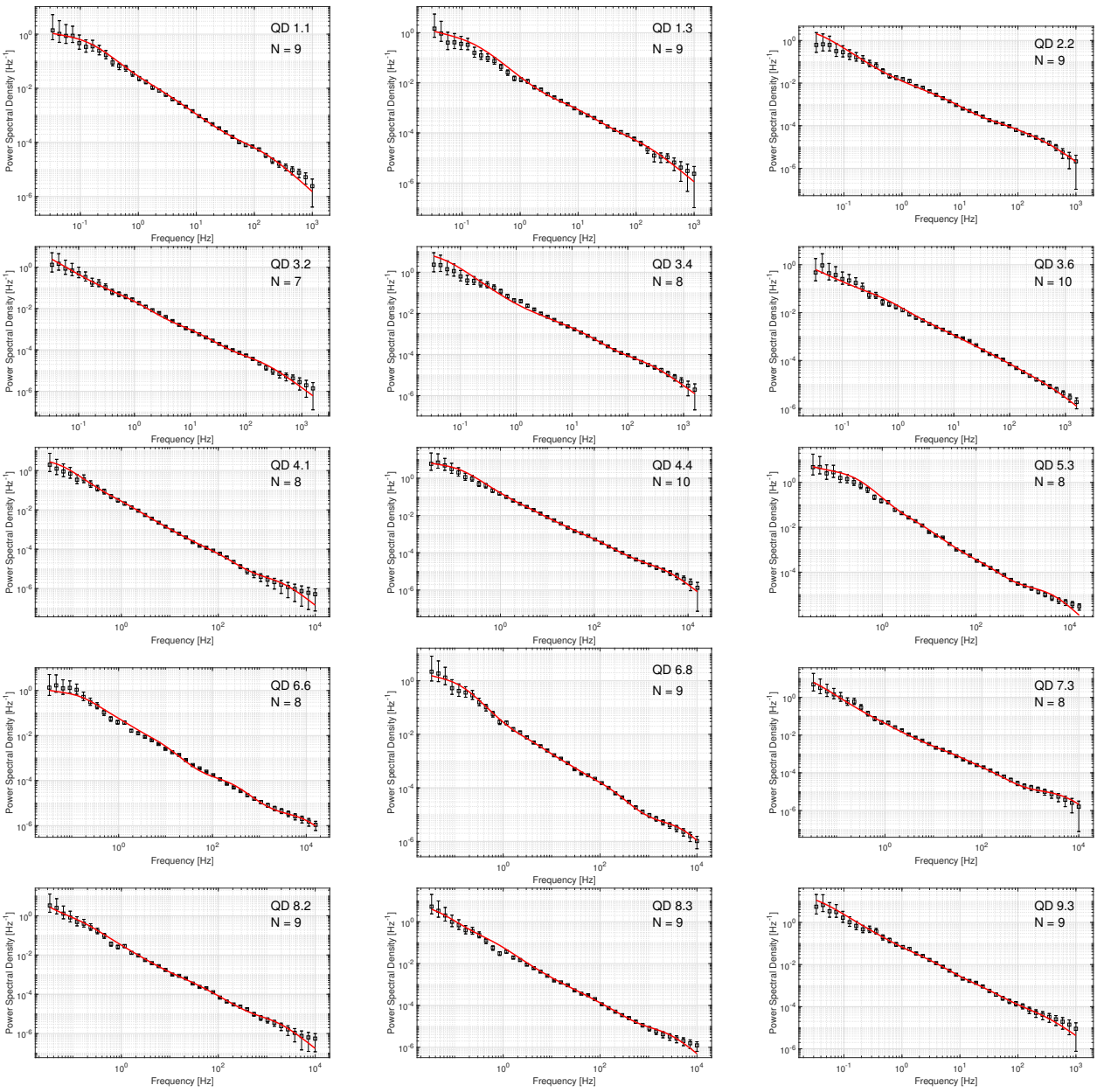

Figure S10: Estimated power spectral density (black squares) model fits (red thin line) for the set of experiments with CdSeS/ZnS single quantum dots

Supplementary note 11: Theoretical prediction of the FLID

In the theoretical model the fluorescence lifetime τ_Σ of the particular configuration Σ is determined as:

$$\tau_\Sigma = \frac{1}{k_r + k_t(\Sigma)} \tag{97}$$

It follows from Eq. (74) that the PLQY of this configuration is connected with τ_Σ by a simple linear relation:

$$Y_\Sigma = \frac{k_r}{k_r + k_t(\Sigma)} \equiv k_r \tau_\Sigma \tag{98}$$

According to Eq. (88) the mean number of detected photons within one bin that starts from state Σ is given by the following expression:

$$\overline{N}_\Sigma = A\overline{Y}_\Sigma + b; \tag{99}$$

where

$$\overline{Y}_\Sigma = \sum_{\Sigma'} Y_{\Sigma'} \overline{G}_{\Sigma'\Sigma} \tag{100}$$

The probability to detect N photons within the bin obeys the Poisson distribution Eq.(86) with a mean value of $\overline{N}_\Sigma$. As well-known for this distribution the average value of N is:

$$\langle N \rangle = \overline{N}_\Sigma \tag{101}$$

and its dispersion is:

$$\sigma^2_{N_\Sigma} \equiv \langle\langle N^2 \rangle\rangle = \overline{N}_\Sigma \tag{102}$$

where $\langle\langle \dots \rangle\rangle$ is the covariance.

The probability distribution function of the photon delay times within one bin that starts

from the state Σ has the multiexponential form:

$$p_{\Sigma}(t) = \sum_{\Sigma'} \frac{\overline{G}_{\Sigma'\Sigma}}{\tau_{\Sigma'}} \exp\left(-\frac{t}{\tau_{\Sigma'}}\right) \tag{103}$$

Processing the experimental data in Supplementary Note 1 includes fitting the fluorescence decay curve using the maximum likelihood procedure with the double exponent function with the noise background. The analysis of the results of this procedure for the probability distribution function (103) is quite complex. Let's limit ourself to a more simple procedure, namely fitting it with a single exponential function with no background. The data was collected from within several bins that had a fixed number of detected photons N so that total number of collected photons N_t was at least 250. Then the likelihood function's logarithm is:

$$\ln L(\tau) = \sum_i n_i \ln\left(\frac{1}{\tau} \exp\left[-\frac{i\delta}{\tau}\right]\right) + L_0 \tag{104}$$

where n_i is the number of detected photons with a time delay contained within an interval of $(i-1)\delta$ and $i\delta$.

$$\sum_i n_i = N_t \tag{105}$$

The expression for the estimated decay time comes from the first derivative:

$$\frac{\sum n_i}{\hat{\tau}} - \frac{\delta}{\hat{\tau}^2} \sum_i n_i i = 0 \tag{106}$$

Thus, the following estimation of the $\hat{\tau}$:

$$\hat{\tau} = \frac{\delta}{N_t} \sum n_i i \tag{107}$$

The variance of the τ estimation Eq.(111) within the maximal likelihood procedure is

defined by the second derivative of the likelihood logarithm function at point $\hat{\tau}$:

$$\frac{1}{2\sigma_{est}^2} = -\frac{N_t}{\hat{\tau}^2} + \frac{2\delta}{\hat{\tau}^3}\sum_i n_i i \tag{108}$$

which follows

$$\sigma_{est}^2 = \frac{\hat{\tau}^2}{2N_t} \tag{109}$$

From the theoretical model (103) we can find the average values of n_i for the bin that starts from state Σ:

$$\langle n_i \rangle = N_t \delta \sum_{\Sigma'} \frac{\overline{G}_{\Sigma'\Sigma}}{\tau_{\Sigma'}} \exp\left(-\frac{i\delta}{\tau_{\Sigma'}}\right) \tag{110}$$

Substituting to Eq.(107) we get the average value of the $\hat{\tau}$ for the bin:

$$\langle \hat{\tau} \rangle = \sum_{\Sigma'} \overline{G}_{\Sigma'\Sigma}\tau_{\Sigma'} \tag{111}$$

On the other hand, this expression is the mean fluorescence lifetime per bin:

$$\sum_{\Sigma'} \overline{G}_{\Sigma'\Sigma}\tau_{\Sigma'} = \overline{\tau}_{\Sigma} \tag{112}$$

Thus:

$$\langle \hat{\tau} \rangle = \overline{\tau}_{\Sigma} \tag{113}$$

As follows from Eq. (89):

$$\overline{Y}_{\Sigma} = k_r \overline{\tau}_{\Sigma} \tag{114}$$

Substituting to Eq. (88) we get the linear dependence of $\overline{N}_{\Sigma}$ on $\overline{\tau}_{\Sigma}$ in our model:

$$\overline{N}_{\Sigma} = A k_r \overline{\tau}_{\Sigma} + b \tag{115}$$

Meanwhile for all our fits the value of b is much less then 1.

The dispersion of $\hat{\tau}$ comes from n_i values fluctuations. The dispersion of each n_i in our

model is:

$$\langle\langle n_i^2\rangle\rangle = \langle n_i\rangle \tag{116}$$

Applying to Eq.(107) we have:

$$\sigma_f^2 \equiv \langle\langle\hat{\tau}^2\rangle\rangle = \left(\frac{\delta}{N_t}\right)^2 \sum \langle\langle n_i\rangle\rangle i^2 = \left(\frac{\delta}{N_t}\right)^2 \sum \langle n_i\rangle i^2 \tag{117}$$

In the case of the multi-exponent decay (103) it can be written as:

$$\sigma_f^2 = \frac{\delta^3}{N_t} \sum_i \sum_{\Sigma'} \frac{\overline{G}_{\Sigma'\Sigma}}{\tau_{\Sigma'}} \exp\left(-\frac{i\delta}{\tau_{\Sigma'}}\right) i^2 \tag{118}$$

and after summation we get the following expression:

$$\sigma_f^2 = \frac{2}{N_t} \sum \overline{G}_{\Sigma'\Sigma} \tau_{\Sigma'}^2 \tag{119}$$

The total dispersion of the τ value can be found as:

$$\sigma_\tau^2 = \sigma_{est}^2 + \sigma_f^2 = \frac{1}{N_t}\left[\frac{1}{2}\overline{\tau}_\Sigma^2 + 2\sum \overline{G}_{\Sigma'\Sigma}\tau_{\Sigma'}^2\right] \tag{120}$$

An example of the theoretical fluorescence lifetime - intensity distribution is shown in Fig. S11. The $\overline{N}_\Sigma$ dependence on $\overline{\tau}_\Sigma$ Eq.(115) is shown by a red line. For each state Σ (magenta squares) the following are shown: 2σ confidence intervals for $\hat{\tau}$ (horizontal bars), 2σ confidence intervals for N (vertical bars), as well as the confidence regions (colored ellipses). The yellow lines are common tangents for all confidence regions. The thin red ellipse corresponds to the state with the most entities on the photon distribution function. After this processing only the red and yellow lines were left on the fits in Fig. S12.

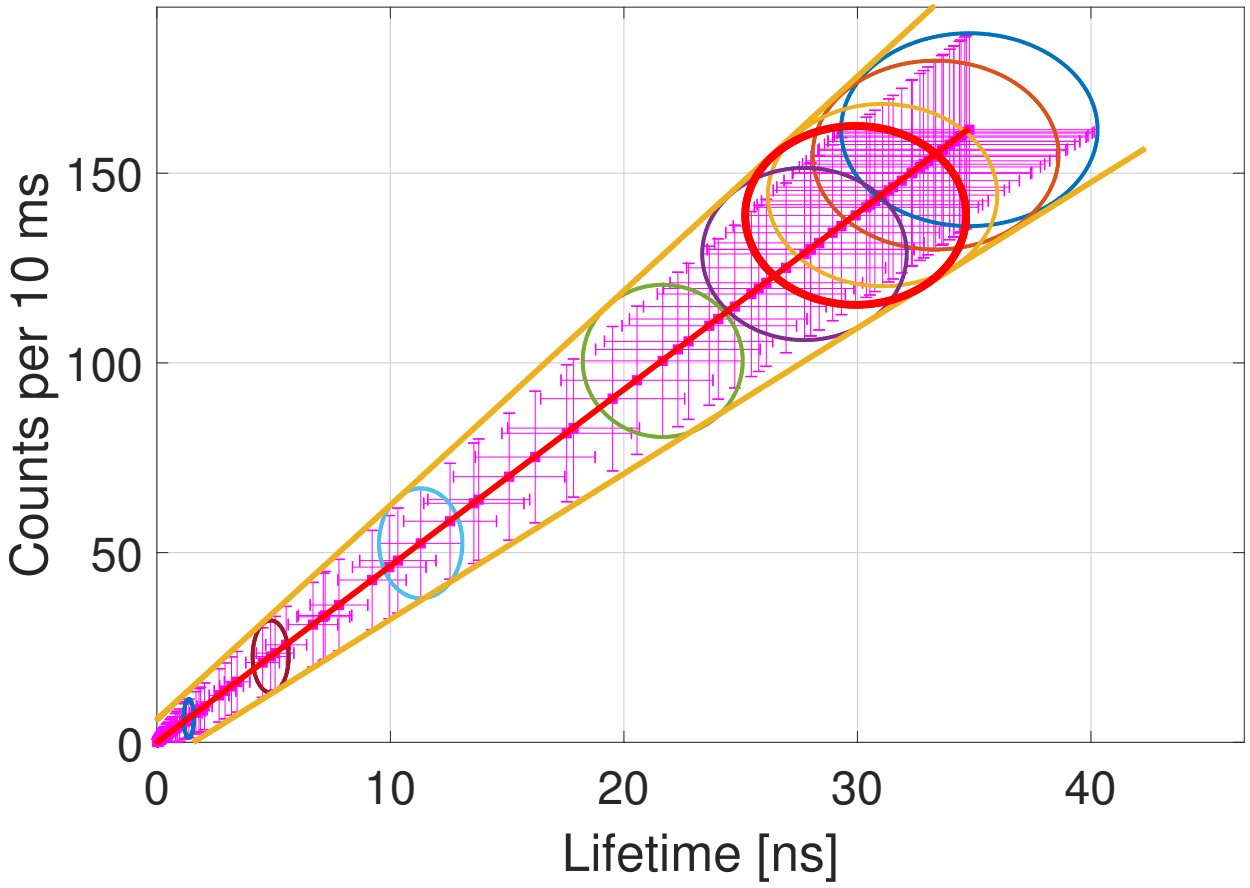

Figure S11: Example of the fluorescence lifetime - intensity distribution resulting from the model with 2σ-confidence interval

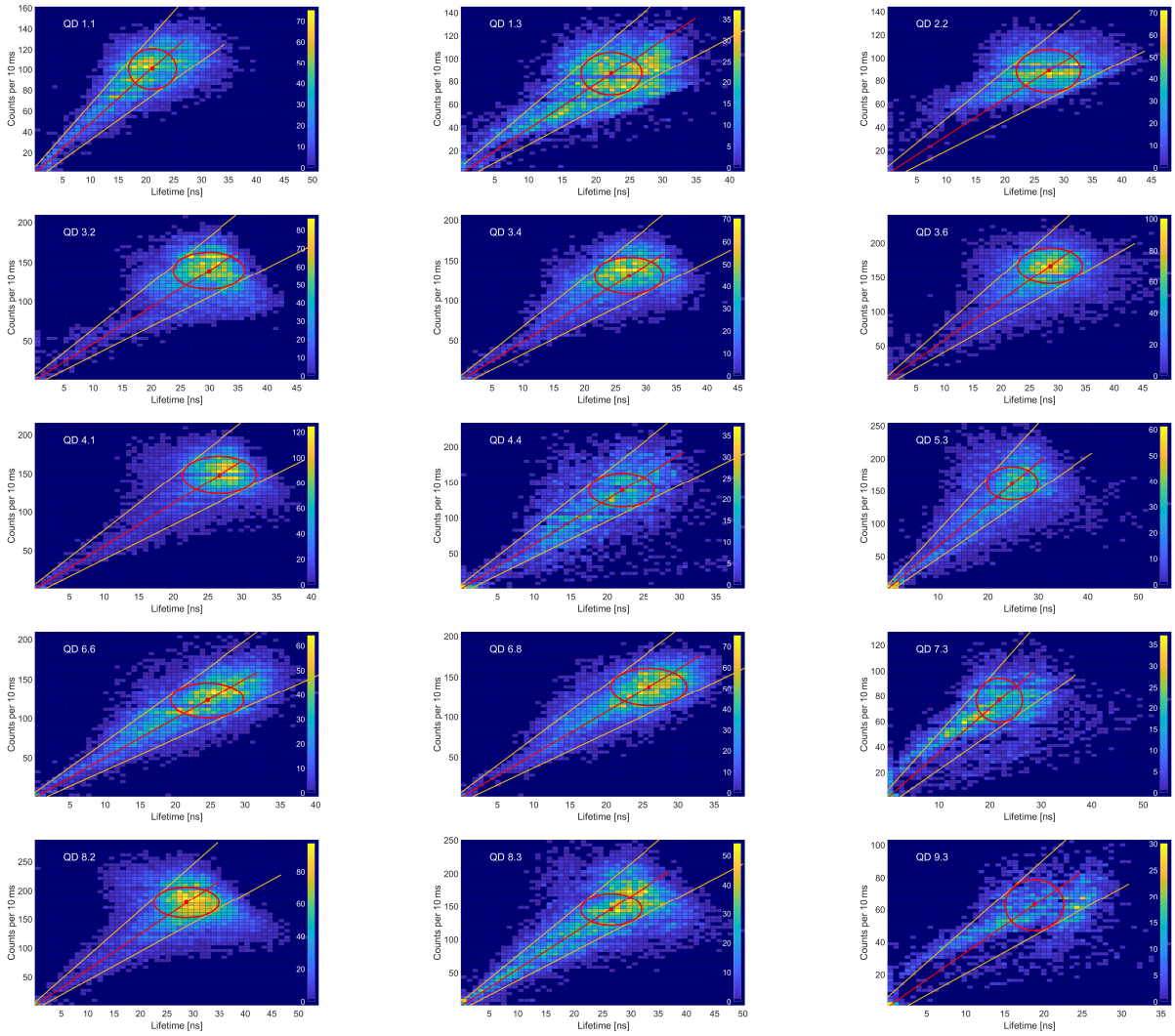

Figure S12: Estimated fluorescence lifetime - intensity distribution (colored histogram) model fits (red thin line) with 2σ confidence regions (yellow thin line) for the set of experiments with CdSeS/ZnS single quantum dots

Supplementary note 12: Photon detection statistics

In order to probe the photon statistics for this model, it is possible to construct several quantities that show the deviation of the photon count from a particular process. To check the deviation from the Poisson process one can calculate the Poisson indicator (for example see[11]):

$$Q(t) = \frac{\langle n^2(t)\rangle - \langle n(t)\rangle^2}{\langle n(t)\rangle} - 1;\ -1 \leq Q(t) < \infty \tag{121}$$

It is easy to see that the indicator is equal to 0 if the process has the Poisson statistics ($\mathrm{var}[n(t)] = \langle n^2(t)\rangle - \langle n(t)\rangle^2 = \langle n(t)\rangle$), if $Q(t) < 0$ then it means that the studied process is sub-Poisson, and super-Poisson otherwise. The long time limit of this indicator is the Mandel's parameter $Q_M = \lim\limits_{t\to\infty} Q(t)$. In our terms, the Poisson indicator can be written as follows:

$$Q(t) = \frac{2k}{t}\int\limits_0^t (t-t')r(t')\mathrm{d}t' \tag{122}$$

where k is the average rate of photon detection that can be expressed as $k = \langle N\rangle/\Delta t$, Δt is the blinking trajectory time bin size, and $\langle N\rangle$ is the average number of photons detected per time bin.

One might calculate the Poisson indicator within the given model by integration of the Eq. (77), so:

$$Q(t) = \frac{2k}{t}\frac{\left(\vec{\boldsymbol{Y}}, \hat{\boldsymbol{H}}(t)\hat{\boldsymbol{Y}}\vec{\boldsymbol{P}}^{\boldsymbol{st}}\right) - t^2/2}{\langle Y\rangle^2} \tag{123}$$

where

$$\hat{\boldsymbol{H}}(t) \equiv \int\limits_0^t (t-t')\hat{\boldsymbol{G}}(t')\mathrm{d}t' = \hat{\boldsymbol{V}}\frac{1}{\hat{\boldsymbol{D}}^2}\left[\exp\left(\hat{\boldsymbol{D}}t\right) - \hat{\boldsymbol{D}}t - 1\right]\hat{\boldsymbol{V}}^{-1} \tag{124}$$

The result for both the theoretical and experimental calculation of the indicator is presented on the Fig. S13a. As can be seen the Poisson factor overcomes a value equal to one on the timescale of hundreds of microseconds and continues to increase to a value of $Q(t) \approx 10^5$ on a timescale close to the maximal switching time of the model, marked by a verical thin line. Such large values of the Poisson indicator means that our process is super-Poisson. The experimentally calculated factor begins to decrease at the tail due to the oscillations of the autocorrelation function around zero at long times, while the model calculated factor reaches its limit of $Q_M \approx 10^5$.

On the other hand, one may also calculate the renewal indicator, the deviation of which from zero is an indicator that the process is not a renewal process. Introduced for the first time by Jianshu Cao,[11] this indicator can be written in the following form:

$$Q_{ev}(t) = \frac{2k}{t}\left[\int_0^t \mathrm{d}t_1 \int_0^{t-t_1} g^{(3)}(t_1+t', t_1)\mathrm{d}t' - \int_0^t \mathrm{d}t_1 \int_0^{t-t_1} g^{(2)}(t_1)g^{(2)}(t')\mathrm{d}t'\right] \tag{125}$$

where $g^{(3)}$ is the third-order correlation function

$$g^{(3)}(t_2, t_1) = \frac{\langle Y(t)Y(t+t_1)Y(t+t_2)\rangle}{\langle Y(t)\rangle^3}$$

The correlation functions can be found within the model as follows:

$$g^{(3)}(t_1+t', t_1) = \frac{\left(\vec{\boldsymbol{Y}}, \hat{\boldsymbol{G}}(t')\hat{\boldsymbol{Y}}\hat{\boldsymbol{G}}(t_1)\hat{\boldsymbol{Y}}\vec{\boldsymbol{P}}^{\boldsymbol{st}}\right)}{\langle Y\rangle^3} \tag{126}$$

$$g^{(2)}(t) = r(t) + 1 = \frac{\left(\vec{\boldsymbol{Y}}, \hat{\boldsymbol{G}}(t)\hat{\boldsymbol{Y}}\vec{\boldsymbol{P}}^{\boldsymbol{st}}\right)}{\langle Y\rangle^2} \tag{127}$$

Now one can introduce the first integral of the $\hat{\boldsymbol{G}}(t)$ matrix:

$$\hat{\boldsymbol{F}}(t) \equiv \int_0^t \hat{\boldsymbol{G}}(t')\mathrm{d}t' = \hat{\boldsymbol{V}} \frac{1}{\hat{\boldsymbol{D}}} \left[\exp\left(\hat{\boldsymbol{D}}t\right) - 1\right] \hat{\boldsymbol{V}}^{-1} \tag{128}$$

It allows us to calculate the next expressions:

$$J_1(t) = \frac{1}{\langle Y \rangle^3} \int_0^t \left(\vec{\boldsymbol{Y}}, \hat{\boldsymbol{F}}(t-t_1)\hat{\boldsymbol{Y}}\hat{\boldsymbol{G}}(t_1)\hat{\boldsymbol{Y}}\vec{\boldsymbol{P}}^{\boldsymbol{st}}\right) \mathrm{d}t_1 \tag{129}$$

$$J_2(t) = \frac{1}{\langle Y \rangle^4} \int_0^t \left(\vec{\boldsymbol{Y}}, \hat{\boldsymbol{G}}(t_1)\hat{\boldsymbol{Y}}\vec{\boldsymbol{P}}^{\boldsymbol{st}}\right) \left(\vec{\boldsymbol{Y}}, \hat{\boldsymbol{F}}(t-t_1)\hat{\boldsymbol{Y}}\vec{\boldsymbol{P}}^{\boldsymbol{st}}\right) \mathrm{d}t_1 \tag{130}$$

and therefore:

$$Q_{ev}(t) = \frac{2k}{t} \left[J_1(t) - J_2(t)\right] \tag{131}$$

The integrals in Eq. (129-130) were numerically calculated to get the $Q_{ev}(t)$ dependence. The result is presented in Fig. S13b. As can be seen, the indicator monotonically increases on the logarithmic scale until the TLS largest switching timescale, which is marked with a black line, and then it starts to decrease to zero, which is the limit for long periods for this indicator. On average time scales the indicator takes on a large positive value, which means our model describes a process that is very different from a renewal process.

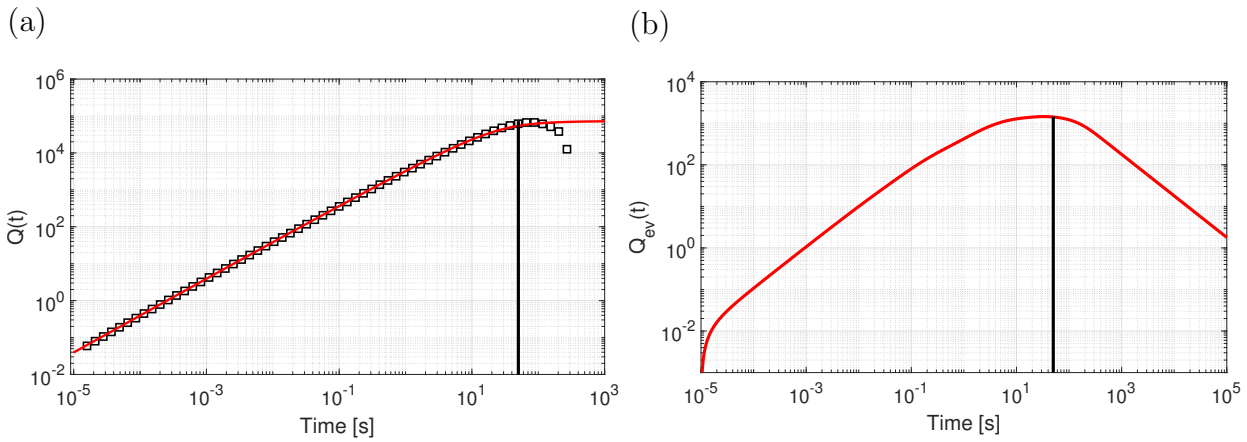

Figure S13: (a) Poisson indicator obtained from the experimental autocorrelation function (black squares) and from the theory (red line). (b) The renewal indicator (red line) obtained from the theory. Vertical lines in the both panels show the maximal characteristic timescale used in the model. Calculations were carried out using the experimental data and model parameters of the experimental set 3.2.

References

(1) Frantsuzov, P. A.; Marcus, R. A. Explanation of quantum dot blinking without the long-lived trap hypothesis. *Physical Review B* **2005**, *72*, 155321.

(2) Frantsuzov, P. A.; Volkán-Kacsó, S.; Jankó, B. Model of Fluorescence Intermittency of Single Colloidal Semiconductor Quantum Dots Using Multiple Recombination Centers. *Physical Review Letters* **2009**, *103*, 207402.

(3) Gilbert, E. N.; Pollak, H. O. Amplitude distribution of shot noise. *The Bell System Technical Journal* **1960**, *39*, 333–350.

(4) Jenkins, G. M.; Watts, D. G. *Spectral analysis and its applications*; San Francisco: Holden-Day, 1968.

(5) Percival, D. B.; Walden, A. T. *Spectral Analysis for Physical Applications*; Cambridge University Press, 1993.

(6) Blackman, R. B.; Tukey, J. W. The measurement of power spectra from the point

of view of communications engineering — Part I. *The Bell System Technical Journal* **1958**, *37*, 185–282.

(7) Nuttall, A. Some windows with very good sidelobe behavior. *IEEE Transactions on Acoustics, Speech, and Signal Processing* **1981**, *29*, 84–91.

(8) Frantsuzov, P. A.; Volkán-Kacsó, S.; Jankó, B. Universality of the Fluorescence Intermittency in Nanoscale Systems: Experiment and Theory. *Nano Letters* **2013**, *13*, 402–408.

(9) Barzykin, A. V.; Frantsuzov, P. A.; Seki, K.; Tachiya, M. Solvent effects in nonadiabatic electron-transfer reactions: Theoretical aspects. *Advanves in Chemical Physics* **2002**, *123*, 511–616.

(10) Gopich, I. V.; Szabo, A. *Theory and Evaluation of Single-Molecule Signals*; World Scientific Publishing Co. Pte. Ltd, 2008; Chapter 6, pp 181–244.

(11) Cao, J. Correlations in Single Molecule Photon Statistics: Renewal Indicator. *The Journal of Physical Chemistry B* **2006**, *110*, 19040–19043, PMID: 16986901.